Nuclear Engineering and Technology 51 (2019) 977–986

Contents lists available at ScienceDirect

Nuclear Engineering and Technology

journal homepage: www.elsevier.com/locate/net

Original Article

Improvement of the MARS subcooled boiling model for a vertical upward flow

Tae-Wook Ha, Jae Jun Jeong*, Byong-Jo Yun

School of Mechanical Engineering, Pusan National University, Busan, 46241 South Korea

ARTICLE INFO

Article history:
Received 14 November 2018
Received in revised form
14 December 2018
Accepted 3 January 2019
Available online 5 January 2019

Keywords:
Subcooled boiling
Net vapor generation
Wall evaporation
Effects of inlet liquid velocity and hydraulic diameter

ABSTRACT

In the thermal-hydraulic system codes, such as MARS and RELAP5/MOD3, the Savannah River Laboratory (SRL) model has been adopted as a subcooled boiling model. It, however, has been shown that the SRL model cannot take into account appropriately the effects of inlet liquid velocity and hydraulic diameter on axial void fraction development. To overcome the problems, Ha et al. (2018) proposed a modified SRL model, which is applicable to low-pressure and low-Pe conditions ($P < 9.83$ bar and $Pe \leq 70{,}000$) only. In this work, the authors extended the modified SRL model by proposing a new net vapor generation (NVG) model and a wall evaporation model so that the new subcooled boiling model can cover a wide range of thermal-hydraulic conditions with pressures ranging from 1.1 to 69 bar, heat fluxes of 97–1186 kW/m^2, Pe of 3600 to 329,000, and hydraulic diameters of 5–25.5 mm. The new model was implemented in the MARS code and has been assessed using various subcooled boiling experimental data. The results of the new model showed better agreements with measured void fraction data, especially at low-pressure conditions.

1. Introduction

Subcooled boiling in a heated channel is characterized by local boiling adjacent to the heated surface although the bulk liquid is subcooled. The accurate prediction of the void fraction in the subcooled boiling region is very important for nuclear safety since it has significant influences on the mass flow rate, the onset of two-phase flow instability and, the heat transfer characteristics in a nuclear reactor core.

Subcooled boiling initiates at the onset of nucleate boiling (ONB) point, where the wall superheat is sufficiently high to cause bubble nucleation. As shown in Fig. 1, the subcooled boiling region in a vertical upward flow is divided into two regions, i.e., a "highly subcooled" and a "low subcooled" region [1]. In the highly subcooled region, the generated bubbles do not grow further and remain attached to the heated wall due to rapid condensation with surrounding highly subcooled liquid. In this region, the void fraction is very low and, thus, can be neglected. In the low subcooled region, the void fraction increases significantly starting from the point of net vapor generation (PNVG), which represents the transition from high to low subcooled boiling region. In most of the best-estimate thermal-hydraulic system codes, such as RELAP5/MOD3.3 [2], MARS 3.1 [3], TRACE [4], and CATHARE [5], the subcooled boiling is assumed to occur from the PNVG.

The subcooled boiling model usually consists of several sub-models; the PNVG model, a wall evaporation model, an interfacial condensation model, etc. The wall evaporation model calculates the vapor generation rate at a heated surface. The amount of condensation of the generated bubbles by the surrounding subcooled liquid is calculated by the interfacial condensation model. Among them, studies on the PNVG has been widely conducted over the past 50 years. Kroeger and Zuber [6] showed that the ability to predict the PNVG is very important for accurate prediction of void fraction. Kennedy et al. [7] described that the PNVG can be also used as a conservative estimate for the onset of flow instability (OFI) [8]. In the study of Saha and Zuber [9], a new NVG correlation was suggested by dividing the subcooled boiling region into thermally controlled (low-velocity) and hydrodynamically controlled (high-velocity) regions based on the Peclet number (Pe). It has been known that the correlation is one of the best models to predict PNVG with a wide range of thermal-hydraulic conditions [10]. The correlation has been still used in the system codes, such as RELAP5/MOD3 and MARS, and has also been used for the prediction of OFI [11].

* Corresponding author.
E-mail address: jjjeong@pusan.ac.kr (J.J. Jeong).

https://doi.org/10.1016/j.net.2019.01.001

Nomenclature

C_n	coefficients in a series expansion
$c_{p,f}$	specific heat capacity of the liquid phase (J/kg·K)
D_h	hydraulic diameter of a channel (m)
g	acceleration due to gravity (m/s^2)
G	mass flux (kg/m^2·s)
h	enthalpy (J/kg)
h_{fg}	latent heat of vaporization (J/kg)
k	thermal conductivity (W/m·k)
$\dot{m}$	mass flow rate (kg/s)
Nu'	modified Nusselt number $= \frac{q_w D_h}{k_f} \frac{c_{pf}}{h_{fg}}$
P	pressure (Pa, bar)
Pe	Peclet number $= \frac{G D_h c_{p,f}}{k_l}$
Pr	Prantl number $= \frac{c_{pf}\mu}{k_f}$
P_h	heated perimeter (m)
q_w	wall heat flux (W/m^2)
r_0	tube radius
Re	Reynolds number $= \frac{G D_h}{\mu}$
T	temperature (K)
u	velocity (m/s)
V	volume of a control volume (m^3)
X_{eq}	thermodynamic equilibrium quality
z	coordinate along a heated channel (m)

Greek symbols

α	average void fraction
Γ	wall vapor generation rate per unit volume (kg/m^3·s)
ρ	density (kg/m^3)
σ	surface tension (N/m)

Subscripts

f	liquid phase
g	gas phase
in	inlet condition
sat	saturation
sub	subcooling
w	wall

However, some deficiencies of the Saha-Zuber's correlation have been continuously reported over the past 30 years. Rogers et al. [12] and Bibeau [13] showed the effect of the liquid inlet velocity for their experimental data under low pressure (~150 kPa) and low velocities (<0.5 m/s) conditions. They pointed out that the Saha-Zuber's correlation does not take into account the velocity effect for the low-velocity region ($Pe \leq 70{,}000$). In the study of Ha et al. [14], it was also shown that the effect of hydraulic diameter is not considered properly. Furthermore, an issue related to the criterion ($Pe = 70{,}000$) for the transition between the low-to-high velocity has also raised in some literature. Kalitvianski [15] proposed the criterion of $Pe = 36{,}400$ for the transition and an adjusted version of the Saha-Zuber correlation was proposed using the KIT experiments [16]. Ha et al. [14] presented a new criterion using a dimensionless velocity, which is defined by the inlet liquid velocity normalized by the bubble rise velocity and proposed a new NVG correlation for $Pe \leq 70{,}000$. However, the proposed NVG correlation could not completely replace the Saha-Zuber model due to the limited application range.

In the RELAP5/MOD3 and MARS codes, the wall evaporation model of Lahey's, so-called the Lahey's mechanistic model [17], has been used until early 2000s. However, the model has some limitations for predicting void fraction at low-pressure conditions because the model has been validated under high-pressure conditions only. To overcome this limitation, Thurston [18] empirically modified the Saha-Zuber NVG model and the Lahey's model using the low-pressure subcooled boiling experiments in annular channels. The package of the two modified models is called "*Savannah River Laboratory (SRL) model*," and has been adopted as a default model in RELAP5/MOD 3.3 [19] and MARS 3.1.

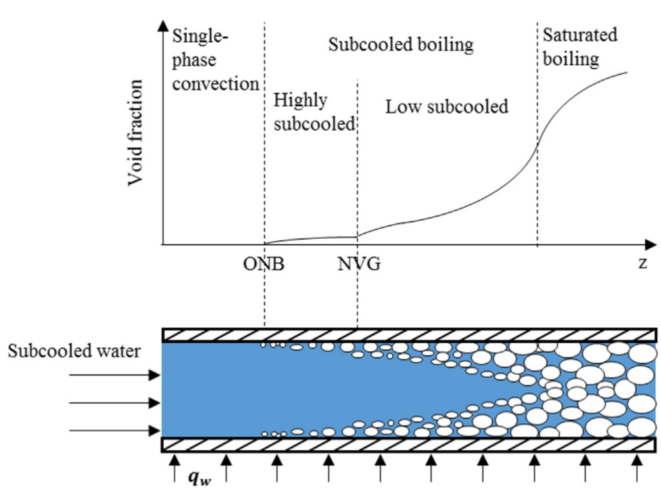

Fig. 1. Axial void fraction in subcooled boiling.

In this study, an improved subcooled boiling model is proposed to replace the SRL model. In Section 2, the SRL model and its deficiencies are summarized. In Section 3, a NVG correlation, which is based on the local Nusselt number for the single-phase laminar and turbulent flows, is proposed and the SRL wall evaporation model is also modified. In Section 4, the package of the proposed models has been assessed using a wide range of experimental data.

2. Subcooled boiling model of MARS-KS

The MARS-KS code is a best-estimate thermal-hydraulic system code, which has been developed from the consolidated version of the RELAP5/MOD3.2 and COBRA-TF [20–23]. It has been further improved and validated for the use of regulatory purposes.

In the MARS-KS code, the SRL model has been used as a subcooled boiling model. In the following sub-sections, the SRL model and its deficiencies are presented.

2.1. The SRL model

The wall evaporation model in the SRL model, which calculates the bubble generation rate on a heated wall surface, is based on Lahey's model [17]. Due to the limitation [24–26] of Lahey's model, Thurston [18] has modified the model to be applicable to low-pressure. The modified model is called the SRL wall evaporation model and, it was summarized as:

$$\Gamma_{w,SRL} = \frac{q_w A_w}{V h_{fg}} \left(\frac{1}{1+\varepsilon_{SRL}}\right)\{M + F_{SRL}\}, \tag{1}$$

where $\Gamma_{w,SRL}$ is the wall vapor generation rate, q_w is the wall heat flux, A_w is the heated area, V is the volume of a control volume, h_{fg} is the latent heat of vaporization, and ε_{SRL} and F_{SRL} is given by:

$$\varepsilon_{SRL} = \frac{\rho_f}{\rho_g} \frac{\left[h_{f,sat} - min\left(h_f, h_{f,sat}\right)\right]}{h_{fg}} F_{eps}, \tag{2}$$

$$F_{SRL} = F_{press}(F_{gam} - M), \tag{3}$$

where F_{eps} and F_{press} and are pressure dependent multipliers. F_{gam} is the fifth order function of M, which is an empirical formula based on the experimental data. They are given as:

$$F_{eps} = \min\left[1.0, \frac{1.0}{0.97 + 38.0 \times exp\left[-\left(\frac{P}{6.894\times10^3} + 60.0\right)/42\right]}\right], \tag{4}$$

$$F_{press} = \frac{1.0782}{1.015 + exp\left[\left(\frac{P}{6.894\times10^3} - 140.75\right)/28\right]}, \tag{5}$$

$$F_{gam} = \min\left[1.0,\ 0.0022 + 0.11M - 0.59M^2 + 8.68M^3 - 11.29M^4 + 4.25M^5\right], \tag{6}$$

where $M = \frac{\min(h_f, h_{f,sat}) - h_{cr}}{h_{f,sat} - h_{cr}}$,where h_{cr} is the bulk liquid enthalpy at the PNVG. The modified Saha-Zuber NVG correlation for h_{cr} was derived from the following correlations:

$$Nu = \frac{q_w D_h}{k_f(T_{sat} - T_{PNVG})} = 455 \text{ for } Pe \le 70,000, \tag{7}$$

$$St = \frac{Nu}{Pe} = \frac{q_w}{Gc_{p,f}(T_{sat} - T_{PNVG})} = 0.0055 - 0.0009 \times F_{press} \text{ for } Pe > 70,000, \tag{8}$$

where $Pe = Re \cdot Pr$.

In the correlations, Pe is used to determine the division between thermally ($Pe \le$ 70,000) and hydro-dynamically ($Pe >$ 70,000) controlled region. $Pe =$ 70,000 is the criterion for the low- and high-velocity regions. Eqs. (7) and (8) can be rewritten in terms of h_{cr}:

$$h_{cr} = \begin{cases} h_{f,sat} - \frac{1}{455} Nu' h_{fg} \text{ for } Pe \le 70,000, \\ h_{f,sat} - \frac{1}{0.0055 - 0.0009 \times F_{press}} \left(\frac{Nu'}{Pe}\right) h_{fg} \text{ for } Pe > 70,000, \end{cases} \tag{9}$$

where $Nu' = \frac{q_w D_h}{k_f} \frac{c_{pf}}{h_{fg}}$.

It is noted that the modified Saha-Zuber model satisfies the continuity at $Pe =$ 70,000. Therefore, the modified model can cause numerical instabilities around $Pe =$ 70,000. In the RELAP5/MOD3 and MARS codes, the SRL model in Eq. (1) through (9) has been adopted as a default model for the subcooled boiling.

2.2. Deficiencies of the SRL model

The SRL model showed deficiencies for the low-velocity region ($Pe \le 70,000$), as reported in Ha et al. [14]. They plotted the experimental void fraction (α) versus the thermal-equilibrium quality (X_{eq}) substituted for the heated channel length (z), using a one-dimensional energy balance equation:

$$X_{eq}(z) = \frac{\left(h_{in} + \frac{q_w P_h z}{\dot{m}}\right) - h_{f,sat}}{h_{fg}}. \tag{10}$$

From this transformation, the deficiency related to the inlet liquid velocity was revealed for the simulation of the subcooled boiling in the MARS code. They also reported the deficiency with respect to the hydraulic diameter. The deficiencies can be described as follows:

- Fig. 2(a) and (b) show α *vs*. X_{eq} of the experiments and the corresponding calculation results under similar heat flux conditions, respectively. In the experimental data, the effect of inlet liquid velocity on axial void fraction development can be clearly observed and, however, the MARS code cannot capture this trend at all. The problem is due to Eq. (1) through (9), which do not involve the fluid veloicity as an input variable.
- Fig. 3(a) and (b) show that the axial void fraction is under-predicted or over-predicted when the hydraulic diameter D_h is relatively small or large based on 12.7 mm (0.5 inch), respectively. This may be due to the fact that the SRL model is based on experimental data with D_h of 12.7 mm (used for the equivalent diameter of fuel rod assembly).

In our study, the SRL model has also been assessed using the experimental data [27,28] for the high-velocity region ($Pe > 70,000$). As shown in Fig. 4(a) and (b), the calculated PNVG showed considerable differences with to the experimental PNVG for $Pe > 70,000$.

An issue related to the criterion between the low-and high-velocity region has also raised in the literature [14,15,29]. The authors presented Peclet numbers lower than 70,000 as the criterion because the Saha-Zuber correlation cannot predict PNVG well, especially for the low-velocity region. The NVG correlations of the authors are summarized in Table 1. Ha et al. [29] fitted again the data cited by Saha and Zuber and, then, proposed a modified Saha-Zuber's correlation. Therefore, the problems mentioned above cannot be solved by using the correlation of Ha et al. The correlations of Ha et al. and Kalitvianski [14,15] also have limitations for application to wide ranges of D_h or Pe and, thus, cannot replace the SRL NVG correlations of Eqs. (9a) and (9b).

3. Improvement of the SRL model

The applicable range of the SRL model is the same as the correlation of Ha et al. [29] in Table 1. To develop an improved correlation which can overcome the limitations of the SRL model, we have collected a lot of subcooled boiling experimental data that can cover a wide range of thermal-hydraulic conditions. These include the experiments by Zeitoun [30], Mcleod [31], Donevski and Shoukri [32], Dimmick and Selander [28], Evangelisti and Lupoli [33], Kim et al. [27], Bibeau [13], Yun et al. [34], Lee et al. [35], Umekawa et al. [36], Ferrell and Bylund [37], Rouhani [38], and Christensen [39]. Thermal hydraulic conditions of these experiments are listed in Table 2.

In this section, we proposed a new NVG correlation and, empirically modified the SRL wall evaporation model based on the study of Ha et al. [14]. The MARS nodalization used for the modification is shown in Fig. 5. It consists of two time-dependent volumes (TDVs), two single volumes (SVs) at the inlet and outlet of the heated section, and a pipe and a heat structure for the heated section. The number of nodes for the heated section was 10 or 20 nodes depending on the distribution of void fraction. The inlet

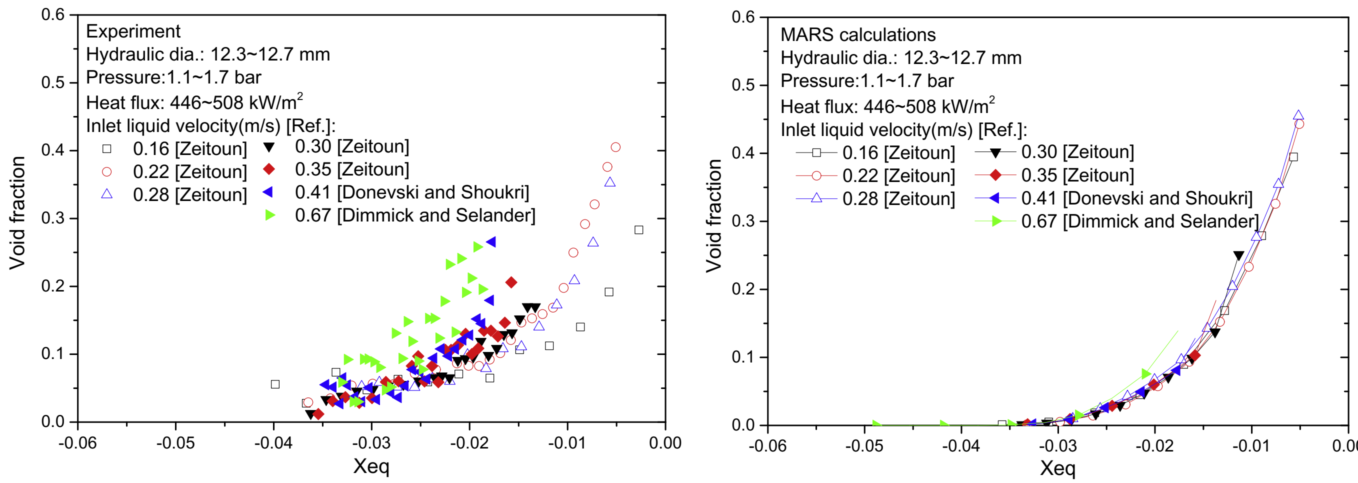

(a) Experimental data (b) The MARS calculations

Fig. 2. Experimental data and calculations: The effect of inlet liquid velocity.

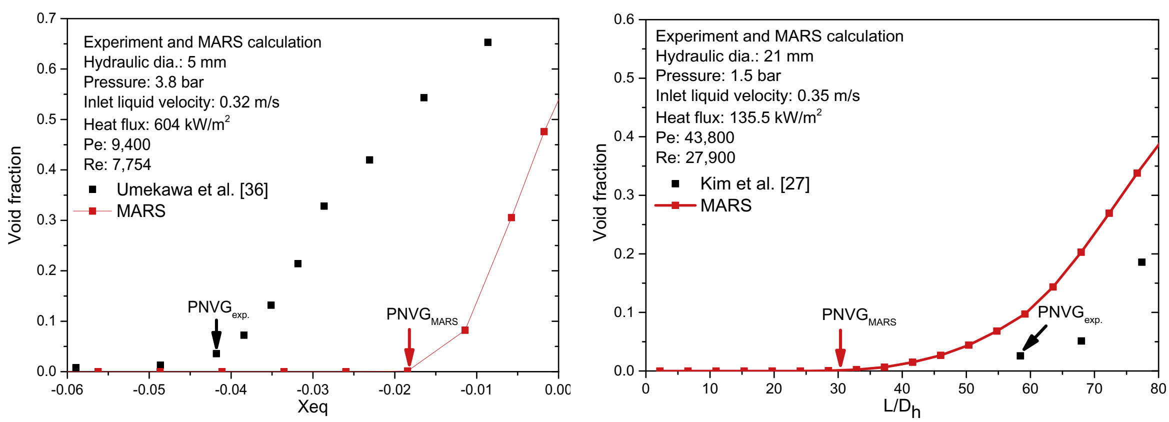

(a) D_h= 5 mm (b) D_h= 21 mm

Fig. 3. Experimental and calculated data: The effect of D_h.

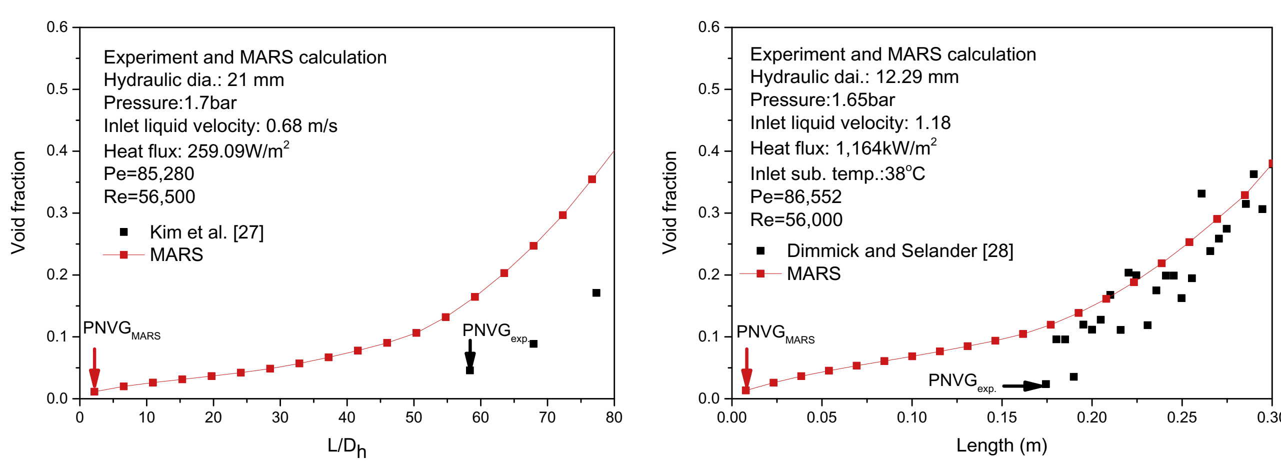

Fig. 4. Experimental and calculated data for $Pe > 70,000$.

liquid temperature and mass flow rate are specified at the inlet time-dependent volume and junction, respectively. The system pressure is specified at the outlet time-dependent volume.

3.1. Proposal of a new NVG correlation

A lot of studies related to PNVG have been conducted over

Table 1
NVG correlation of the authors [14,15,29].

Authors	Formula of models	Applicable range
Ha et al. [29]	$h_{cr} = \begin{cases} h_{f,sat} - \frac{1}{918.5}\left(\frac{q_w D_h c_{p,f}}{k_f}\right) Pe^{0.08} & \text{for } Pe < 52,000 \\ h_{f,sat} - 34.84\left(\frac{q_w D_h c_{p,f}}{k_f}\right)\left(\frac{1}{Pe}\right)^{0.876} & \text{for } Pe \geq 52,000 \end{cases}$	$P = 1.01 \sim 138$ bar, $D_h = 4.0 \sim 13$ mm, $Pe = 5,000 \sim 345,000$.
Kalitvianski [15]	$h_{cr} = \begin{cases} h_{f,sat} - \frac{5}{455}\left(\frac{q_w D_h c_{p,f}}{k_f}\right) & \text{for } Pe \leq 36,400 \\ h_{f,sat} - \frac{2 \times 70,000^{0.4}}{0.0065}\left(\frac{q_w D_h c_{p,f}}{k_f}\right)\left(\frac{1}{Pe}\right) & \text{for } Pe > 36,400 \end{cases}$	$P = 44 \sim 110$ bar, $D_h = 11.7$ mm, $Pe = 32,000 \sim 311,000$.
Ha et al. [14]	$h_{cr} = \begin{cases} h_{f,sat} - 7.29 h_{fg} Bo^{0.8203} & \text{for } u^*_{L.P.} \leq 1.55 \\ h_{f,sat} - 32.94 h_{fg} Bo^{0.9016} & \text{for } u^*_{L.P.} > 1.55 \end{cases}$ where $Bo = \frac{q_w}{G h_{fg}}$ and $u^*_{L.P.} = \frac{u_i}{1.18 \times \{g\sigma(\rho_f - \rho_v)\}^{0.25} / \rho_f^{0.5}}$	$P = 1.1 \sim 9.8$ bar, $D_h = 5 \sim 21$ mm, $Pe = 3,600 \sim 70,000$.

Table 2
Experimental conditions used for the improved subcooled boiling model.

Experiment	No. of tests	Press. (bar)	Heat flux (kW/m^2)	Mass flux ($kg/m^2 \cdot s$)	Inlet subcooled temp. (K)	Pe	Geometry Type	D_h(mm)
Zeitoun [30]	25	1.1–1.7	210–706	161–412	11–31	12,000 ~32,500	Annular	12.7
Mcleod [31]	19	1.55	297–1186	65–480	30–76	3600 ~26,600	Annular	8.9
Donevski and Shoukri [32]	6	1.5–2.1	481–733	315–450	19–29	25,000 ~35,500	Annular	12.7
Dimmick and Selander [28]	4	1.65	472–1164	620–1116	28–61	48,400 ~86,600	Tube	12.3
Evangelisti and Lupoli [33]	3	1.2	446–885	607–1410	24–25	22,600 ~52,600	Annular	6
Kim et al. [27]	4	1.3–1.7	97–259	334–653	12–15	44,000 ~86,000	Annular	21
Bibeau [13]	6	1.55	300–980	67–252	17–79	3800 ~14,200	Annular	9.1
Yun et al. [34]	5	1.6–1.9	374–566	1104–2075	17–29	175,200 ~329,300	Annular	25.5
Lee et al. [35]	2	1.1–1.5	375–377	668–684	12–16	83,000 ~85,000	Annular	20
Umekawa et al. [36]	2	3.8–5.0	604–626	300	62–72	9400 ~18,900	Tube	5,10
Ferrell and Bylund [37]	6	4.1–8.2	246–530	440–542	28–62	33,600 ~41,000	Tube	11.9
Rouhani [38]	18	9.8–50	300–902	79–533	10–39	8100 ~45,200	Annular	13
Christensen [39]	3	28–69	355–497	880–940	12–14	125,100 ~135,900	Rectangular	17.8
Total	103	1.1–69	97–1186	65–2075	10–79	3600–329,300	Tube, Rect., Annular	5–25.5

several decades. Some of them [12,40,41] have developed the NVG models by postulating that the region before the PNVG is a single-phase flow. They also presented that the PNVG was considerably affected by the temperature distribution away from the heated wall. Based on these studies, we deduce that the PNVG would be closely related to the local Nusselt number Nu for single-phase laminar and turbulent flows.

The correlations for the local Nu have already been presented in many paper and books [42–45]. For the laminar flow, the conservation of energy equation is mathematically solved to obtain the local Nu. In the case of a laminar flow in a circular tube with a constant heat flux [45], the local Nu is presented as follows:

$$Nu = \frac{2}{\frac{11}{24} + \sum_{n=1}^{\infty} C_n exp\left(\frac{-\beta_n^2 x}{r_0}\frac{1}{Pe}\right) R_n(1)}. \quad (11)$$

For the fully developed laminar flow, the exponential term in Eq. (11) disappears and Nu becomes a constant 4.36. Generally, the constant depends on the types of the flow cross-section, boundary condition, etc. For a fully-developed turbulent flow, the correlation proposed by Dittus and Boelter [46] has been widely used. It is given by:

$$Nu = 0.0243 Re^{0.8} Pr^{0.4} \quad (12)$$

It is noted that Nu in Eq. (7) is constant and Nu in Eq. (8) is a function of Re and Pr. The SRL NVG correlations are similar to the local Nu of Eqs. (11) and (12), respectively. Therefore, a new NVG model could be proposed using the formulations of Eqs. (11) and (12).

In the SRL NVG model, Pe = 70,000 is used as a criterion between the low-and high-velocity regions and it corresponds to $Re = \sim 40,000$ at a low-pressure condition. However, Eq. (12) can be used for $Re \geq 10,000$. It seems that the NVG correlations divided by Pe = 70,000 shows poor predictions because of the inadequate criterion. As listed in Table 1, some authors [15,29] have proposed a criterion lower than Pe = 70,000, e.g. 36,400 or 52,000. Besides

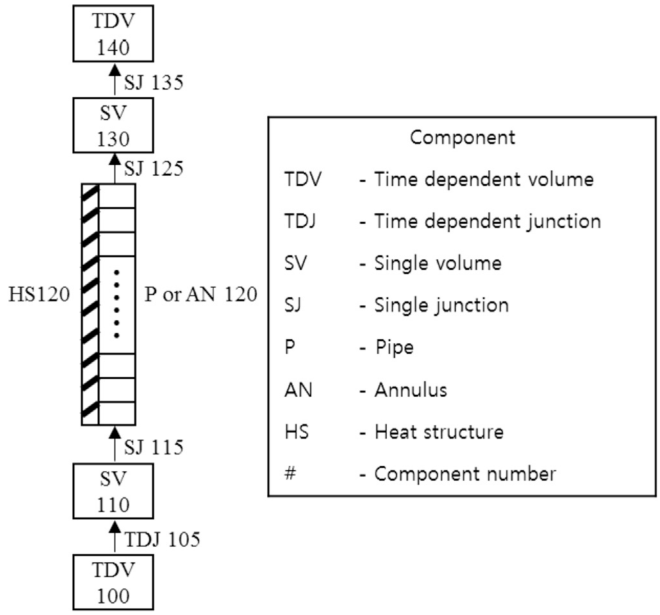

Fig. 5. MARS nodalization of the experimental setup.

these, Ha et al. [14] proposed a dimensionless inlet liquid velocity as a criterion for the low-and high-velocity regions. It was based on the observation of many experimental data. This criterion corresponds to Re of ~13,000 when D_h is 12.7 mm. It can be rewritten as:

$$u^* = \frac{\dot{m}/\rho_f A}{1.53\left(\frac{g\sigma(\rho_f-\rho_v)}{\rho_f^2}\right)^{0.25}} = 1.2, \tag{13}$$

where $\dot{m}/\rho_f A$ represents the inlet liquid velocity and the denominator is the bubble rise velocity.

The PNVGs in the 103 experimental cases in Table 2 were fitted for the low-and high-velocity regions:

$$Nu = \frac{q_w D_h}{k_f(T_{sat} - T_{PNVG})} = \frac{1}{0.0901 - 0.0893\exp\left(-158\frac{1}{Pe}\right)} \text{ for } u^* \leq 1.2, \tag{14}$$

$$Nu = \frac{q_w D_h}{k_f(T_{sat} - T_{PNVG})} = 1.09Pe^{0.5833} \text{ for } u^* > 1.2, \tag{15}$$

The thermal equilibrium quality at the PNVG, $x_{eq,PNVG}$, is given by:

$$x_{eq,PNVG} = -\frac{c_{pf}(T_{sat} - T_{PNVG})}{h_{fg}}. \tag{16}$$

Eqs. (14) and (15) can be expressed as:

$$x_{eq,PNVG} = \begin{cases} -\{0.0901 - 0.0893exp(-158/Pe)\}Nu' \text{ for } u^* \leq 1.2, \\ -0.9176Nu'\left(\frac{1}{Pe}\right)^{0.5833} \text{ for } u^* > 1.2, \end{cases} \tag{17}$$

The critical enthalpy is obtained by

$$h_{cr} = h_{f,sat} + x_{eq,PNVG}h_{fg}. \tag{18}$$

Figs. 6 and 7 compare the experimental $X_{eq,PNVG}$ with the calculated ones by the SRL and the new models for the low- and high-velocity regions, respectively. For each region, the root mean square error (RMSE) is obtained by:

$$\text{RMSE} = \sqrt{\frac{\sum_i^n \left|X_{eq,\ exp.,i} - X_{eq,cal.,i}\right|}{n}}.$$

As shown in Table 3, the RMSE by the new model is considerably reduced compared with the RMSE by the SRL model. The reduction of relative RMSE is 33% and 29% for the low- and high-velocity regions, respectively. However, Eq. (23) do not satisfy the continuity at $u^* = 1.2$. To resolve this problem, a linear interpolation was adopted between $u^* = 1.1$ and 1.2.

3.2. Modification of the wall evaporation model

In the SRL wall evaporation model of Eq. (3), F_{gam} in F_{SRL} plays an important role in determining the amount of wall evaporation, especially under low-pressure conditions. F_{gam} is the fifth-order function of M, which considers the enthalpy only, and it does not take into account the effects of inlet liquid velocity and D_h at all. In the work of Ha et al. (2018), F_{gam} was modified as a function of enthalpy and inlet liquid velocity. In this work, the authors modified F_{gam} as a function of enthalpy, inlet liquid velocity, and D_h to resolve the deficiencies mentioned in Section 2.2. The basic function of the modified F_{gam} was designed as:

$$F_{gam} = \min\left[0.9M^2 + 0.1M + f(u^*, D^*)sin(\pi M),\ 1.0\right]. \tag{19}$$

To find appropriate coefficients for $f(u^*, D^*)$, we simulated the subcooled boiling experiments in Table 2 several times using the MARS. Finally, the function $f(u^*, D^*)$ was obtained for the low- and high-velocity regions, respectively. A linear interpolation was also adopted between $u^* = 1.1$ and 1.2 to avoid a discontinuity:Where

$$f(u^*, D^*) = \begin{cases} \min\left[0.09196u^{*0.266}D^{*2}, 1.0\right] & for\ u^* \leq 1.1, \\ \text{Linearly interpolated} & for\ 1.1 < u^* \leq 1.2, \\ \min\left[0.43837(u^* - 1.2)^{0.545}D^{*2}, 1.0\right] & for\ u^* > 1.2, \end{cases} \tag{20}$$

$$D^* = \frac{D_{ref}}{D_h}, \text{ and } D_{ref} = 12.7 \text{ mm}.$$

The new models were implemented into MARS-KS1.5 instead of the SRL model.

4. Assessment of the modified subcooled boiling model

The 103 subcooled boiling experiments in Table 2 were simulated using the modified MARS code. The results of the original and modified MARS codes are compared with the experimental data.

4.1. Simulation results for the selected experiments

Fig. 8 shows the simulation results of the selected experiments in Section 2.2. The comparison of Fig. 2(a) and (b) and 8 shows that the modified MARS code can represent the effect of inlet liquid velocity very well in contrast to the original MARS code. Fig. 9(a) and (b) show the simulation results for a small and large D_h,

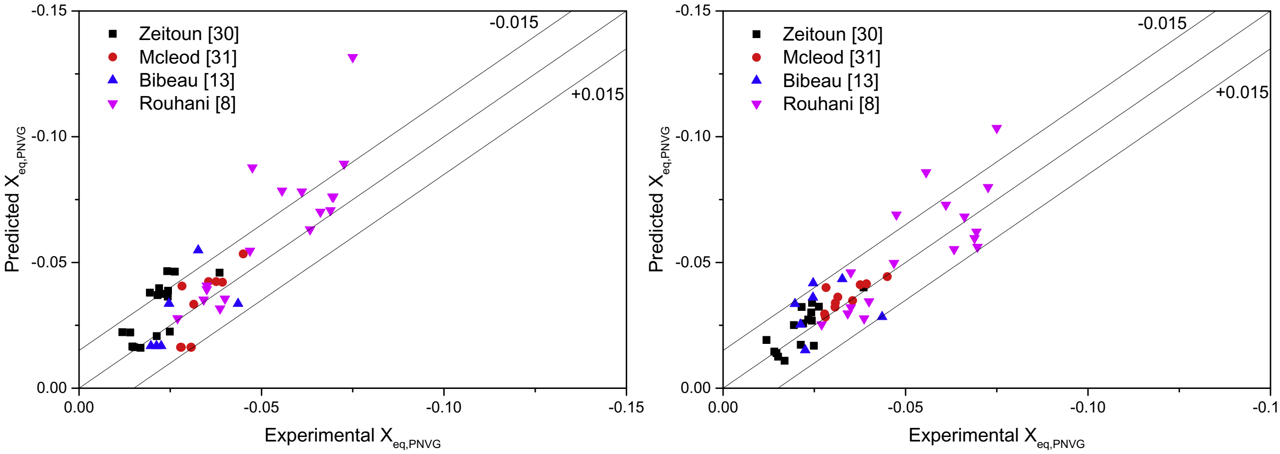

(a) The SRL model (b) The new NVG model

Fig. 6. Comparison of the experimental and predicted $x_{eq,PNVG}$ for $u^* \leq 1.2$.

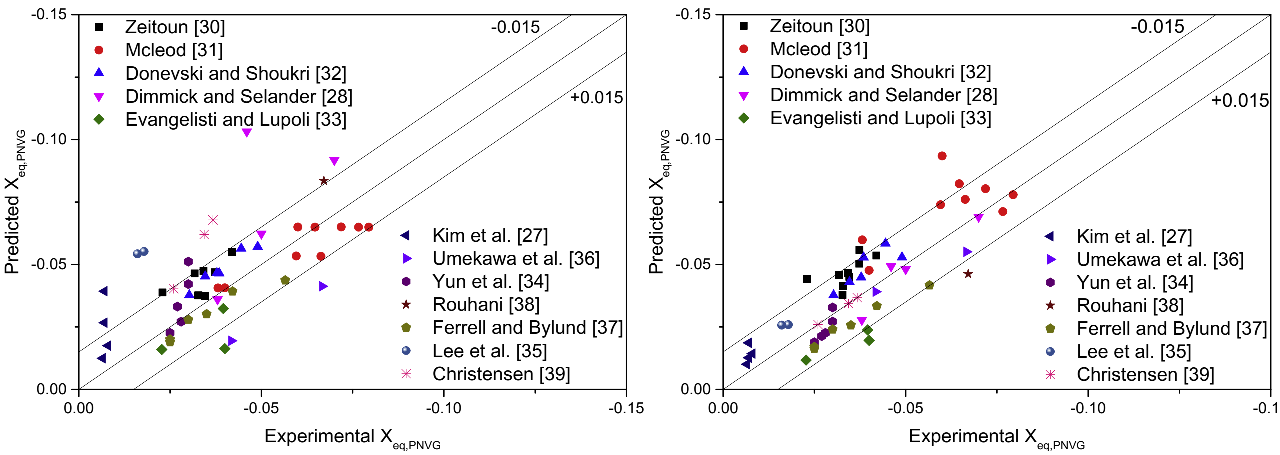

(a) The SRL model (b) The new NVG model

Fig. 7. Comparison of the experimental and predicted $x_{eq,PNVG}$ for $u^* > 1.2$.

Table 3
The RMSE of $X_{eq,PNVG}$ by the original SRL and the new models.

Range	The SRL model	The new model
$u^* \leq 1.2$	0.015	0.010
$u^* > 1.2$	0.017	0.012

respectively. The modified code leads to better prediction of the PNVG for both small and large diameter pipes. The distribution of the axial void fraction was also better predicted. Fig. 10 (a) and (b) shows the simulation results for $Pe > 70,000$. As shown in Fig. 10 (a), the prediction of PNVG was improved and, the distribution of axial void fraction was also predicted well due to the modified F_{gam} considering D_h. Fig. 10 (b) also shows better predictions of the PNVG.

Fig. 11 is the results of numerical subcoled boiling experiments, where the inlet water velocity gradually changed with a fixed wall heat flux. It can be seen that the modified SRL model leads to a smooth transition at the low- and high-veolcity boundary.

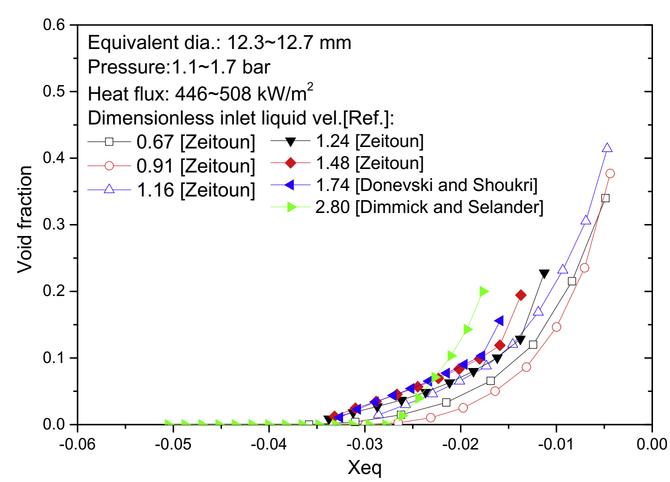

Fig. 8. The calculation results of the modified MARS: The effect of inlet liquid velocity.

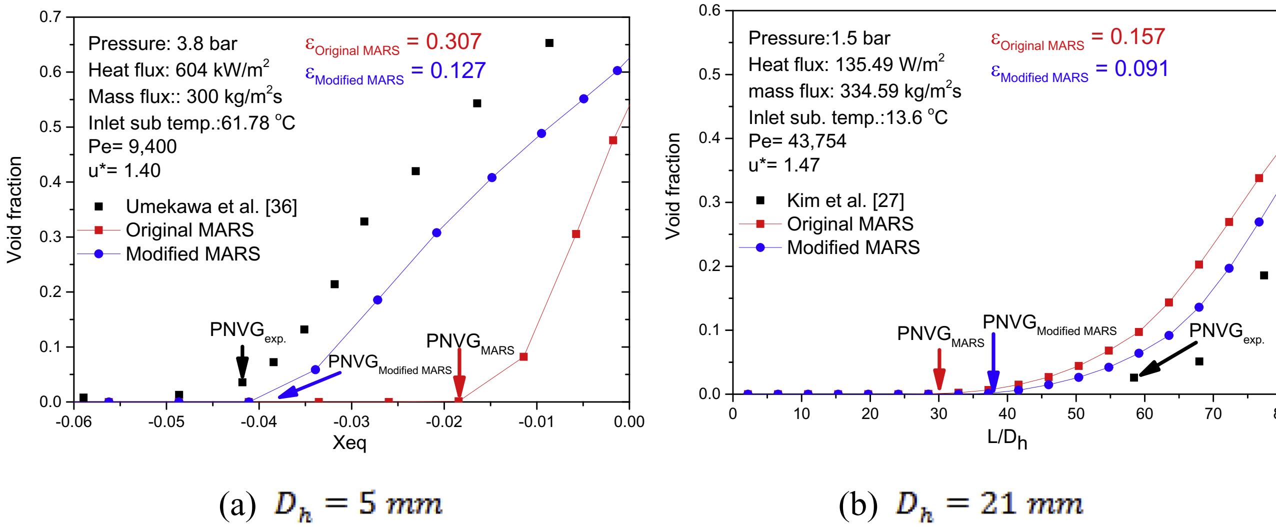

Fig. 9. The calculation results of the original and the modified MARS: The effect of D_h.

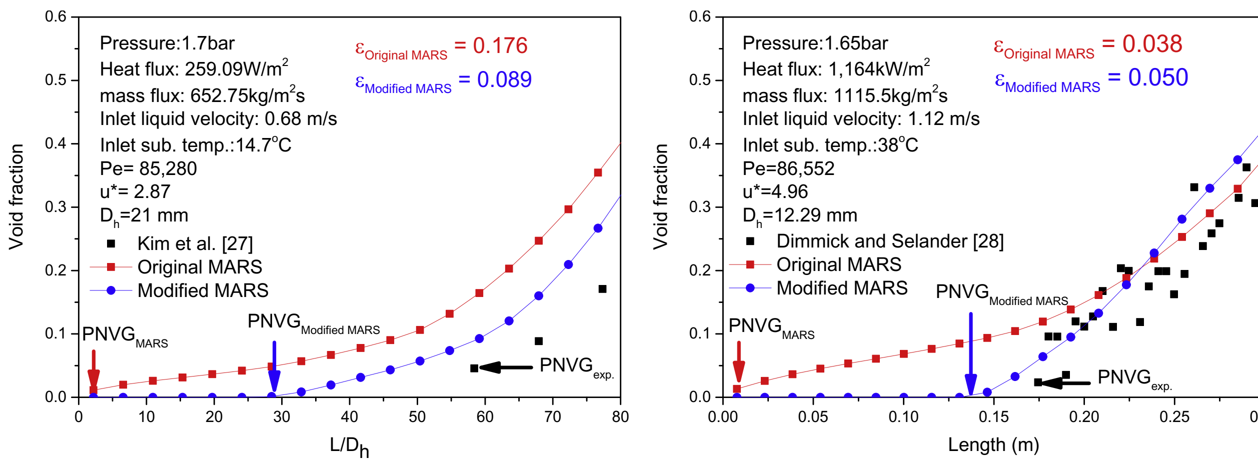

Fig. 10. Simulation results of the modified MARS code for $Pe > 70,000$.

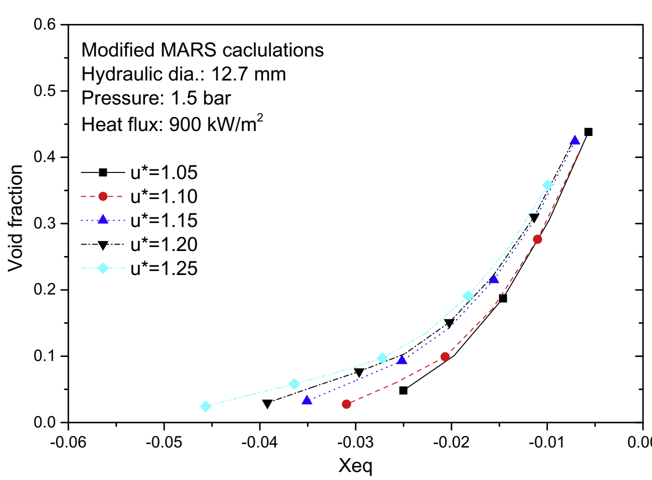

Fig. 11. The results of numerical experiments to show a smooth transition as for u^*.

4.2. Quantitative assessment of the modified model

For the overall assessment, the average void fraction error was derived. In the MARS code, the subcooled boiling is assumed to occur from the PNVG. It is known that considerable uncertainty exists in experiments to determine the PNVG [47,48]. For this assessment, the PNVG is assumed as the point, where the measured void fraction increases up to 0.05. An average of the absolute void fraction errors (ε) from the PNVG to the end of the test section was obtained for each experimental case:

$$\varepsilon = \frac{1}{n}\sum_{i=1}^{n}\left|\alpha_{exp,i} - \alpha_{cal,i}\right|, \tag{21}$$

where n is the number of measurement points, $\alpha_{exp,i}$ is a measured void fraction, and $\alpha_{cal,i}$ is a calculated void fraction at the position of experimental measurement, which is obtained by a linear interpolation of the void fractions at two adjacent computing cells.

As shown in Fig. 12(a) and (b), the measured void fraction (a total of 923 data points) was compared with the predicted void fraction by the original and the modified codes, respectively. In the original code, a total of 207 data points were out of the ranges of

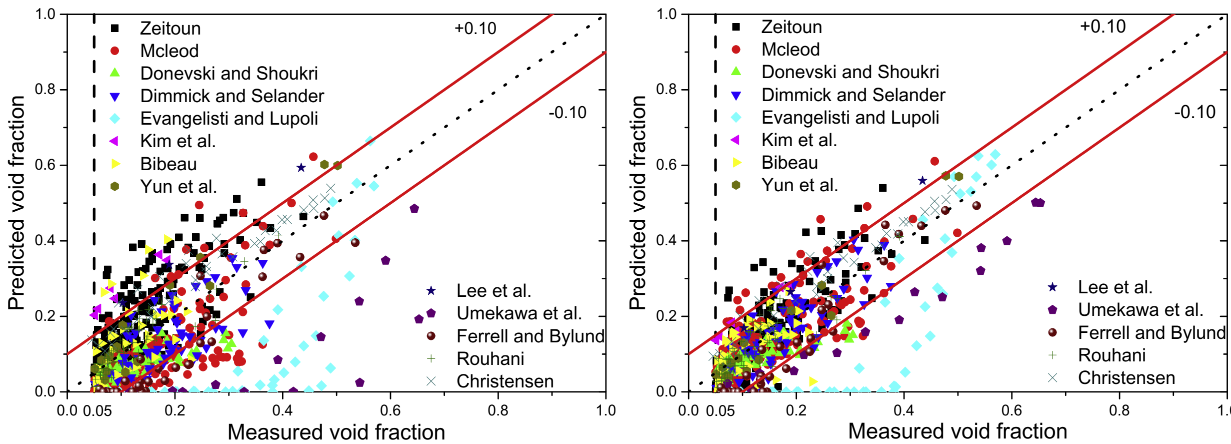

(a) The original MARS (b) The modified MARS

Fig. 12. Comparison of the measured and predicted void fraction data.

Table 4
Average void fraction error for the 13 experiments.

Experiment	No of tests (Data points)	ε_{mean}	
		Original MARS	Modified MARS
Zeitoun [30]	25 (308)	0.076	0.053
Mcleod [31]	19 (239)	0.080	0.051
Donevski and Shoukri [32]	6 (62)	0.061	0.041
Dimmick and Selander [28]	4 (59)	0.069	0.041
Evangelisti and Lupoli [33]	3 (44)	0.212	0.165
Kim et al. [27]	4 (6)	0.173	0.093
Bibeau [13]	6 (39)	0.065	0.056
Yun et al. [34]	5 (14)	0.044	0.029
Lee et al. [35]	2 (3)	0.147	0.086
Umekawa et al. [36]	2 (16)	0.263	0.145
Ferrell and Bylund [37]	6 (30)	0.099	0.078
Rouhani [38]	18 (67)	0.030	0.031
Christensen [39]	3 (36)	0.071	0.052
Total	103 (923)	0.107	0.071

$\pm$0.1 void fraction error, but 119 cases only in the modified code. The average ε (ε_{mean}) for each experiment is summarized in Table 4. The modified MARS code shows considerably reduced ε_{mean} for each experiment compared to the original code except for the Rouhani's experiment. For the experiment, the original and modified code provide almost the same results. This is due to the fact that, as the pressure increases, the effect of the correction factors in the SRL wall evaporation model tends to disappear and the PNVG becomes less important in predicting the void fraction than at low pressure. The absolute void fraction error averaged for thirteen experiments is reduced by 3.6%, which is equivalent to a 34% reduction in the relative error. Thus, it can be said that the modified model yields a significant improvement in the prediction of subcooled boiling.

5. Conclusions

In the thermal-hydraulic system codes, such as MARS and RELAP5, the SRL model has been adopted as a subcooled boiling model. It was shown that the subcooled boiling model in the MARS code cannot appropriately consider the effects of inlet liquid velocity and hydraulic diameter on axial void fraction development. To resolve the problems, Ha et al. (2018) suggested a modified SRL model and, however, the model was not sufficient to replace the original SRL model because of the limited application range ($P < 9.83$ bar and $Pe \leq 70,000$).

In this work, the authors have collected more subcooled boiling experimental data, which can cover a wide range of thermal-hydraulic conditions. Then, a new NVG correlation and a wall evaporation model were proposed. The new NVG correlation is based on the local Nusselt number for the laminar and turbulent flow of single phase, which were theoretically more sound. The new wall evaporation model takes into account the effects of inlet liquid velocity and hydraulic diameter. Meanwhile, the work of Ha et al. (2018) did not consider the effects of higher inlet water velocity and hydraulic diameter. The modified code has been assessed using the 103 sets of experiments that cover a wide range of Peclet number and pressure conditions. It was shown that the modified MARS code can yield better predictions of both PNVG and axial void fraction development than the original code especially for low-pressure conditions. The results of the modified MARS code for the experiments show about 34% reduction of relative average void fraction error in comparison to those of the original MARS code.

Acknowledgments

This work was supported by the Nuclear Safety Research Program through the Korea Foundation Of Nuclear Safety (KoFONS) using the financial resource granted by the Nuclear Safety and Security Commision of the Republic of Korea (No. 1305011).

References

[1] J.G. Collier, Convective Boiling and Condensation, McGraw-Hill, New York, 1981.
[2] RELAP5-3D© Code Development Team, RELAP5-3D© Code Manual Volume IV: Models and Correlations, Idaho National Lab., 2005. INEEL-EXT-98-00834.
[3] KAERI, MARS Code Manual Volume I: Code Structure, System Models and Solution Methods, Korea Atomic Energy Research Institute, 2009. KAERI/TR-2812.
[4] J.W. Spore, J.S. Elson, S.J. Jolly-Woodruff, T.D. Knight, J.C. Lin, R.A. Nelson, K.O. Pasamehmetoglu, R.G. Steinke, C. Unal, TRAC-M/Fortran 90(Version 3.0) Theory Manual, Los Alamos Lab, 2000. NUREG/CR-6724.
[5] D. Bestion, The physical closure laws in the CATHARE code, Nucl. Eng. Des. 124 (3) (1990) 229–245.
[6] P.G. Kroeger, N. Zuber, An analysis of the effects various parameters on the average void fractions in subcooled boiling, Int. J. Heat Mass Tran. 11 (2) (1968) 211–233.
[7] J.E. Kennedy, G.M. Roach, M.F. Dowling, S.I. Abdel-Khalik, S.M. Ghiaasiaan, S.M. Jeter, Z.H. Quershi, The onset of flow instability in uniformly heated horizontal microchannels, J. Heat Tran. 122 (1) (2000) 118–125.
[8] P. Saha, M. Ishii, N. Zuber, An experimental investigation of the thermally induced flow oscillations in two-phase systems, J. Heat Tran. 98 (4) (1976) 616–622.
[9] P. Saha, N. Zuber, Point of net vapor generation and vapor void fraction in subcooled boiling, in: 5th International Heat Transfer Conference, Tokyo, 1974.
[10] S.C. Lee, S.G. Bankoff, A comparison of predictive models for the onset of significant void at low pressures in forced-convection subcooled boiling, KSME Int. J. 12 (3) (1998) 504–513.
[11] A. Ghione, B. Noel, P. Vinai, C. Demazière, Criteria for onset of flow instability in heated vertical narrow rectangular channels at low pressure: an assessment study, Int. J. Heat Mass Tran. 105 (2017) 464–478.
[12] J.T. Rogers, M. Salcudean, Z. Abdullah, D. Mcleod, D. Poirier, The onset of significant void in up-flow boiling of water at low pressure and velocities, Int. J. Heat Mass Tran. 30 (11) (1987) 2247–2260.
[13] E.L. Bibeau, Experimental Investigation of Subcooled Void Growth for Upflow and Downflow at Low Velocities and Low Pressure, PhD Thesis, University of British Columbia, 1988.
[14] T.W. Ha, J.J. Jeong, H.Y. Yoon, B.J. Yun, Improvement of the MARS subcooled boiling model for low-pressure, low-Pe flow conditions, Ann. Nucl. Energy 120 (2018) 236–245.
[15] V. Kalitvianski, Qualification of CATHARE 2 V1. 5 Rev. 6 on Subcooled Boiling Experiments (KIT Test), CEA, 2000. SMTH/LMDS/EM/2000-030.
[16] L.S. Sabotinov, Experimental Investigation of Void Fraction in Subcooled Boiling for Different Power Distribution Law along the Channel, PhD Thesis, Moskva in Russian, 1974.
[17] R.T. Lahey, A mechanistic subcooled boiling model, in: 6th International Heat Transfer Conference, Toronto, Canada, 1978.
[18] C.G. Thurston, RELAP5/MOD3 Benchmarks of Low Pressure Subcooled Vapor Voiding in Annular Flow Channels, Babcock & Wilcox Advanced Systems Engineering, 1992. Doc. 51-3001526-00.
[19] U.S. NRC, RELAP5/MOD3.3 Code Manual Volume I: Code Structure, System Models, and Solution Methods, U.S. Nuclear Regulatory Commission, 2010. NUREG/CR-5535/Rev P4-VolI.
[20] S.Y. Lee, J.J. Jeong, S.H. Kim, S.H. Chang, COBRA/RELAP5: a merged version of the COBRA-TF and RELAP5/MOD3 codes, Nucl. Technol. 99.2 (1992) 177–187.
[21] J.J. Jeong, K.S. Ha, B.D. Chung, W.J. Lee, Development of a multi-dimensional thermal-hydraulic system code, MARS 1.3. 1, Ann. Nucl. Energy 26 (18) (1999) 1611–1642.
[22] J.J. Jeong, W.J. Lee, B.D. Chung, Simulation of a main steam line break accident using a coupled 'system thermal-hydraulics, three-dimensional reactor kinetics, and hot channel analysis' code, Ann. Nucl. Energy 33 (9) (2006) 820–828.
[23] B.D. Chung, S.W. Bae, J.J. Jeong, S.M. Lee, Development and Assessment of Multidimensional Flow Models in the Thermal-hydraulic System Analysis Code MARS, Korea Atomic Energy Research Institute, 2005. KAERI/TR—3011/2005.
[24] A.S. Devkin, A.S. Podosenov, RELAP5/MOD3 Subcooled Boiling Model Assessment, U.S. Nuclear Regulatory Commission, 1998. NUREG/IA-0025.
[25] S. Hari, Y.A. Hassan, Improvement of the subcooled boiling model for low-pressure conditions in thermal-hydraulic codes, Nucl. Eng. Des. 216 (1) (2002) 139–152.
[26] B. Končar, B. Mavko, Modelling of low-pressure subcooled flow boiling using the RELAP5 code, Nucl. Eng. Des. 198 (3) (2003) 261–286.
[27] M.O. Kim, S.J. Kim, G.C. Park, Comparison of void fraction profiles in subcooled boiling of low pressure by 3D measurement and MARS calculation, in: Korean Nuclear Society Conference, 2002.
[28] S.R. Dimmick, W.N. Selander, A Dynamic Model for Predicting Subcooled Void: Experimental Results and Model Development, EUROTHERM seminar, Pisa, Italy, 1990.
[29] K.S. Ha, Y.B. Lee, H.C. No, Improvements in predicting void fraction in subcooled boiling, Nucl. Technol. 150 (3) (2005) 283–292.
[30] O.M. Zeitoun, Subcooled Flow Boiling and Condensation, PhD thesis, University of McMaster, 1994.
[31] R.D. Mcleod, Investigation of Subcooled Void Fraction Growth in Water under Low Pressure and Low Flow Rate Conditions, Master thesis, University of Carleton, 1987.
[32] B. Donevski, M. Shoukri, Experimental Study of Subcooled Flow Boiling and Condensation in an Annular Channel, McMaster University, 1989. ME/89/TFRI.
[33] R. Evangelisti, P. Lupoli, The void fraction in an annular channel at atmospheric pressure, Int. J. Heat Mass Tran. 12 (6) (1969) 699–711.
[34] B.J. Yun, B.U. Bae, D.J. Euh, C.H. Song, Experimental investigation of local two-phase flow parameters of a subcooled boiling flow in an annulus, Nucl. Eng. Des. 240 (12) (2010) 3956–3966.
[35] Y.G. Lee, J.W. Yoo, S. Kim, Measurement of local two-phase flow parameters in an annulus under low-pressure subcooled boiling condition, J. KSME (B) 42 (12) (2018) 813–824.
[36] H. Umekawa, S. Nakamura, S. Fujiyoshi, T. Ami, M. Ozawa, Y. Saito, D. Ito, The influence of the heating condition on the void fraction in a boiling channel, Physics Procedia 69 (2015) 599–606.
[37] J.K. Ferrell, D.M. Bylund, Low Pressure Steam-water Flow in a Heated Vertical Channel. Final Report Volume II on a Study of Convection Boiling inside Channels, North Carolina State University, Raleigh, 1966. Dept. of Chemical Engineering.
[38] S.Z. Rouhani, Void Measurements in the Regions of Sub-cooled and Low-quality Boiling, Part I. Low Mass Velocities, AB Atomenergi, 1966. No. AE–238.
[39] H. Christensen, Power-to-void Transfer Functions, PhD Thesis, Massachusetts Institute of Technology, 1961.
[40] S. Levy, Forced convection subcooled boiling—prediction of vapor volumetric fraction, Int. J. Heat Mass Tran. 10 (7) (1967) 951–965.
[41] F.W. Staub, The void fraction in subcooled boiling—prediction of the initial point of net vapor generation, J. Heat Tran. 90 (1) (1968) 151–157.
[42] T.L. Bergman, F.P. Incropera, A.S. Lavine, D.P. Dewitt, Introduction to Heat Transfer, fifth ed., John Wiley & Sons, 2011.
[43] L.C. Burmeister, Convective Heat Transfer, second ed., John Wiley & Sons, 1993.
[44] J.R. Sellars, M. Tribus, J. Klein, Heat Transfer to Laminar Flow in a Round Tube or Flat Conduit: the Graetz Problem Extended, 1954.
[45] R. Siegel, E.M. Sparrow, T.M. Hallman, Steady laminar heat transfer in a circular tube with prescribed wall heat flux, Appl. Sci. Res. Section A 7 (5) (1958) 386–392.
[46] F.W. Dittus, L.M.K. Boelter, University of California Publications on Engineering, University of California Publications in Engineering, vol. 2, 1930, p. 371.
[47] E.L. Bibeau, M. Salcudean, Subcooled void growth mechanisms and prediction at low pressure and low velocity, Int. J. Multiphas. Flow 20 (5) (1994) 837–863.
[48] O. Zeitoun, M. Shoukri, Axial void fraction profile in low pressure subcooled flow boiling, Int. J. Heat Mass Tran. 40 (4) (1997) 869–879.